Continuous SiC fibers-ZrB_2 composites

L. Zoli[a], V. Medri[a], C. Melandri[a], D. Sciti[a]*

[a]CNR-ISTEC, Institute of Science and Technology for Ceramics, Via Granarolo 64, I-48018 Faenza, Italy

*Corresponding author: Diletta Sciti, e-mail: diletta.sciti@istec.cnr.it, phone: +39 0546 699748

E-mails: L. Zoli, luca-zoli@istec.cnr.it, V. Medri, valentina.medri@istec.cnr.it, C. Melandri, cesare.melandri@cnr.it, D. Sciti, diletta.sciti@istec.cnr.it

ABSTRACT

ZrB_2 - continuous SiC fiber composites were prepared by vacuum-bag infiltration and hot pressing, using SiC fabric preforms. Vacuum bag infiltration was effective when unidirectional fiber layers in a 0-90° architecture were infiltrated with an aqueous ZrB_2-rich slurry. Sintering was carried out at temperatures between 1450 and 1600°C to study the effect on densification and microstructural features. With a fiber content of around 50 vol% , the composites had a density of 4 g/cm^3 and final porosities lower than 10 vol%. Flexural strength was measured at room and high temperature in air. Irrespective of the processing temperature, strength values were 150 -170 MPa up to 1200°C and 110 MPa at 1500°C. Short-term oxidation tests were conducted at 1650°C in a bottom-up furnace.

Keywords: ZrB_2, SiC fibers, Ceramic matrix composites, Infiltration, Sintering, UHTCMC

1. Introduction

The development of a new generation of ceramic materials is a priority for enabling operation under extreme conditions. There is an increasing demand for advanced materials with temperature capability over 2000°C for aerospace applications. Ceramic matrix composites (CMCs) based on non-oxide ceramics such as C/SiC possess excellent high-temperature strength, high thermal conductivity, low coefficient of thermal expansion, good thermal shock resistance. However, their poor oxidation resistance restricts their high temperature applications below 1700°C [1,2]. On the other hand Ultra-high temperature ceramics (UHTCs) have been identified as potential candidates for operating in harsh conditions owing to their melting point exceeding 3000°C and their resistance to ablation [3,5] but the low fracture toughness (3-4 MPa.m $^{1/2}$) and low thermal shock

resistance (few hundred degrees) remain major concerns for the application of these materials under severe environments. UHTC- CMCs represent a novel class of materials, which can potentially couple the high oxidation resistance of UHTCs to the damage tolerance of CMCs, provided that a suitable matrix/fiber interface is tailored. In the literature, there is still a limited number of published works concerning the infiltration of SiC preforms with UHTCs. Preliminary work was done by the authors of the present works, using homemade 1D SiC preforms infiltrated with UHTCs slurries based on ZrB_2 [6]. C. J. Leslie et al. have recently studied the fabrication of SiC continuous fiber reinforced composites with HfB_2-SiC powders via polymer infiltration, slurry infiltration and thermal treatment [7]. Another example is the work of Levine et al [8] where 35vol% of SiC fibers were embedded in a ZrB_2-SiC matrix through filament winding and slurry infiltration and subsequently hot pressed. More literature is available on C/C or C/SiC composites. The high temperature oxidation performance of UHTC composites prepared using Cf preforms and a variety of UHTC powder combinations has been recently studied [9,10]. The composites were fabricated by impregnating 2.5 D Cf preforms containing 23 vol% fibers with various UHTC powders (HfB_2, ZrB_2-SiC, HfC, etc) by vacuum impregnation. Their high temperature performance was tested using an oxyacetylene torch test facility with the peak front face temperature being up to 2700°C. Other studies are concerned with C/C composites where the matrix is enriched with up to 30 vol% of various UHTCs phases (ZrB_2, ZrC, etc). These composites are fabricated through different techniques such as slurry infiltration, polymer infiltration, chemical vapor deposition, reactive infiltration etc. [11-15] In this work, continuous SiC fibers preforms were infiltrated with ZrB_2 based aqueous slurries using the vacuum-bag infiltration technique and then sintered by conventional hot pressing. Although the use of hot pressing for densification of CMCs is mentioned in some contributions, results in the open literature are hardly found [9]. Densification, microstructural features and mechanical properties are analyzed.

2. Experimental

The following raw materials were used: -ZrB_2 (Grade B, H.C. Starck, Germany), specific surface area 1.0 m^2/g, particle size range 0.5-6 μm, impurities (wt%): 0.25 C, 2 O, 0.25 N, 0.1 Fe, 0.2 Hf; -$ZrSi_2$ (Japan New Metals Co., LTD, Osaka, Japan) particle size 2-5 μm, impurities (wt%): C>0.15, Fe>0.30, O>1.00; -Tyranno PSA-F17S08PX, Plain waive with 800 fibres/yarn fabric weight 238.7 g/m^2fiber density 3.1 g/cm^3, Tensile Strength 2.19 GPa, Tensile Modulus 369 GPa.

For the matrix of the CMCs, ZrB_2 was mixed with $ZrSi_2$ as sintering aid (20 vol%) on the basis of previous studies [6,14] (see Table 1). The powder mixtures were homogenized through mechanical mixing using ceramic milling media and ethanol, in plastic bottles for 24 h, dried by rotary evaporator and sieved. With those powders mixtures, aqueous slurries were prepared according to previous studies [17]. The composites were fabricated infiltrating the 2D or 1D fabrics with the slurry by hand lay-up. 1-D fabrics, prepared using the same SiC Tyranno fibers (800 fibres/yarn, fabric weight ~120 g/m^2) of 2D-fabrics, were stacked in a 0-90° configuration. Vacuum-bagging was carried out in analogy with the well-established procedures for organic-polymer infiltration, with a subsequent drying at 80°C for 2 h in a conventional air furnace at ambient pressure. At least 30 layers were stacked to produce 3 mm thick plates. Hot pressing cycles were then carried out in the range 1450-1600°C in low vacuum, using a pressure of 20-40 MPa, according to previous densification studies [6,16,18]. After sintering, the composites density was measured by the Archimedes' method. The microstructures were analyzed by field emission scanning electron microscopy (FE-SEM, Carl Zeiss Sigma NTS Gmbh Öberkochen, Germany) and energy dispersive x-ray spectroscopy (EDS, INCA Energy 300, Oxford instruments, UK). X-ray diffraction analyses were carried out using a Bruker D8 Advance apparatus (Bruker, Karlsruhe, Germany). 4-pt bending strength tests were carried out for selected compositions at room temperature, 1200 and 1500°C in air. The specimens, 25 x 2.5 x 2 mm^3, (length by width by thickness, respectively, with no beveling of edges) were fractured using a semi-articulated silicon carbide four-point fixture with a lower span of 20 mm and an upper span of 10 mm in a screw-driven load frame (Instron mod. 6025, Wycombe UK).

Oxidation tests were carried out in a bottom-loading furnace (Nannetti FC18, Faenza, Italy) at 1650°C for 5 minutes on rectangular 13 x 2.5 x 2 mm^3 bars in static air. Specimens were located in the furnace when the maximum temperature was achieved and then removed and air-quenched after the exposure time. The microstructures after oxidation were analyzed by FE-SEM/EDS.

3. Results and Discussion

3.1 Densification and microstructural features

Compositions, sintering cycles, fiber amount and densities of the composites are reported in Table 1. Fiber volumetric amount was determined *a posteriori* on the basis of the initial composition, considering the fabric weight (g/m^2) given by the supplier, number of layers and sample area. The matrix amount was then determined after debonding by subtraction of the total

pellet weight minus the fiber weight. Theoretical densities (see values in Table 1) were calculated using the rule of mixture on the basis of the starting nominal compositions. The SiC-ZrB_2 composites have bulk densities in the range 4-4.2 g/cm^3, with limited porosities, < 10 %. The sintering temperature, between 1450 and 1600°C did not significantly affect the final density, as explained below. A typical x-ray diffraction pattern is displayed for 1D-1600 (densified at 1600°C), and the main crystalline phases are the constituents ZrB_2 and β-SiC, whilst lower reflections belong to $ZrSi_2$ (Fig .1).

Sample label	Fiber Type	Sintering cycle	Fiber volumetric amount	Theoretical density	Bulk Density	Porosity	Flexural strength	Flexural strength 1200°C	Flexural strength 1500°C
			%	g/cm^3	g/cm^3	%	MPa	MPa	MPa
2D-1550 (1)	2D	1550°C/20MPa	~55	4.4	~3.9	~10	21±3	-	-
1D-1450 (2)	1D	1450°C/40MPa	~50	4.5	~4.0	~9	157±4	154±8	114±7
1D-1500 (3)	1D	1500°C/40MPa	~50	4.5	~4.1	~6.5	90±26	172±18	107±35
1D-1550 (4)	1D	1550°C/40MPa	~50	4.5	~4.2	~5	151±20	-	-
1D-1600 (5)	1D	1600°C/40MPa	~50	4.5	~4.2	~5	145±10	136±28	109±14

Table 1: Compositions, sintering aid/cycles, density and porosity and flexural strength of the fabricated composites.

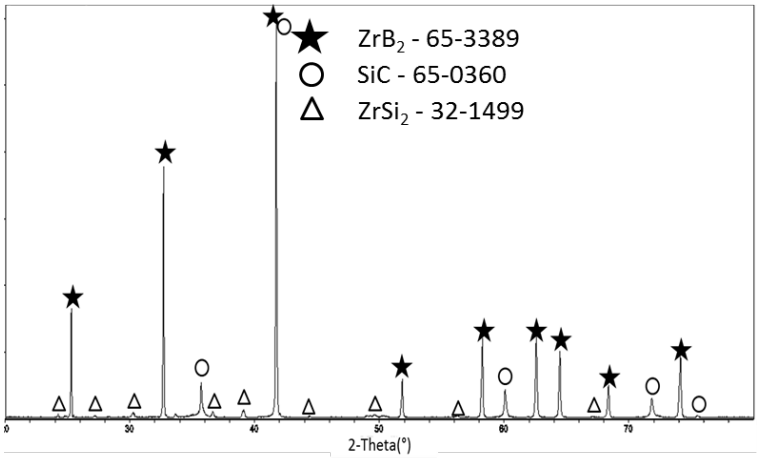

Fig. 1: X-ray diffraction pattern of sample 1D-1600

Fig. 2a, b shows a section of the composite obtained infiltrating the plain waive fabric. It is apparent that the degree of infiltration is very poor. Only the external part of bundles (3 or 4 fibres in depth) were wetted and penetrated by the slurry. Very likely, the tight bonding of the fibers due to the plain weaving did not allow a good penetration of the slurry, nerveless the viscosity was not particularly high (394 cP at 10 s−1, [6]), The poor level of infiltration was not improved by the

densification cycle, despite the formation of liquid phase due to $ZrSi_2$ melting/decomposition is expected at 1550°C. As a result, fully dense matrix layers (see inset in Fig. 2) with thicknesses of 300 μm are overlapped to non-infiltrated fabric layers. Cracks are also evident in matrix-rich regions, very likely caused by the differential shrinkage of the matrix during sintering and thermal expansion coefficient mismatch between matrix and fibers (6.5 10^{-6} $°C^{-1}$ [3], 4.5 10^{-6} $°C^{-1}$ [19], respectively). During sintering, ZrB_2 particles were forced to rearrange and sinter due to liquid phase, whilst the fiber-rich parts were not involved in this process. Due to that the tensional stress arose in the matrix, which led to vertical cracks. Fig. 2b shows a typical fracture surface, with fiber pullout obviously enhanced by the scarce penetration of ceramic slurry in the preform.

As for the composites obtained infiltrating 1D layers, the amount of porosity is lower than 10% (Table 1) and showed the tendency to decrease with increase of the sintering temperature. Pores are due to incomplete sintering in areas where infiltration with ZrB_2 was less effective. The volumetric amount of fibers varied around 50%.

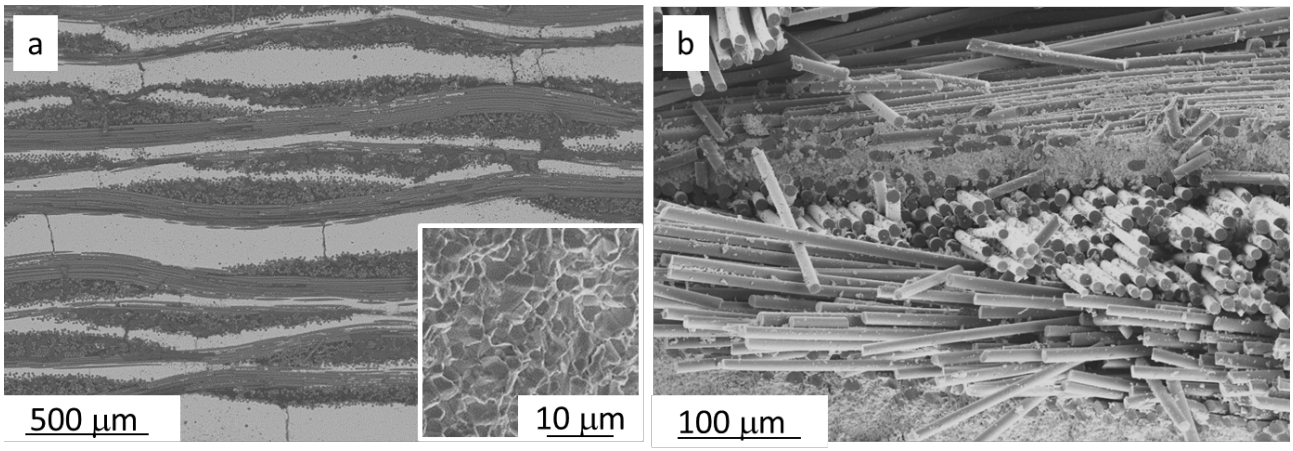

Fig.2: a) Section of the 2D infiltrated samples showing matrix layers overlapped to fiber layers (inset: detail of the matrix), b) fracture surface

Since the stiffness of SiC 2D fabrics hinders the swelling of the bundle and the consequent infiltration, the experiments carried out suggested that preforms with lower fabric weight are suitable for this kind of process allowing fiber spreading and the penetration of the ceramic particles. Fig. 3 shows the typical textural and microstructural features of dense pellets with single infiltrated layers in 0-90°C architecture and sintered at temperatures in the range 1450 and 1600°C (samples 1D-1450, 1500, 1550, 1600). For all of them, the polished section in Fig. 3a demonstrates that the degree of infiltration is much improved compared to the previous case, and at the same time the formation of cracks is reduced, probably due to a better integration between the two

constituent phases. Better infiltration was very likely facilitated by free movement of fiber bundles that were allowed to expand while penetrated by the slurry as well as lower fabric weight (~120 g/m^2) of the 1D preforms. Upon sintering at 1450°C the matrix is almost fully densified and the fibers are well adherent to the matrix. Increasing the sintering temperature led to further reduction of porosity, but also enhanced the reaction at the matrix/fiber interface. On the fracture surface it is apparent that even after sintering at the lowest temperature 1450°C, the degree of fiber pull-out was much reduced compared to sample 2D-1550, Fig. 3b.

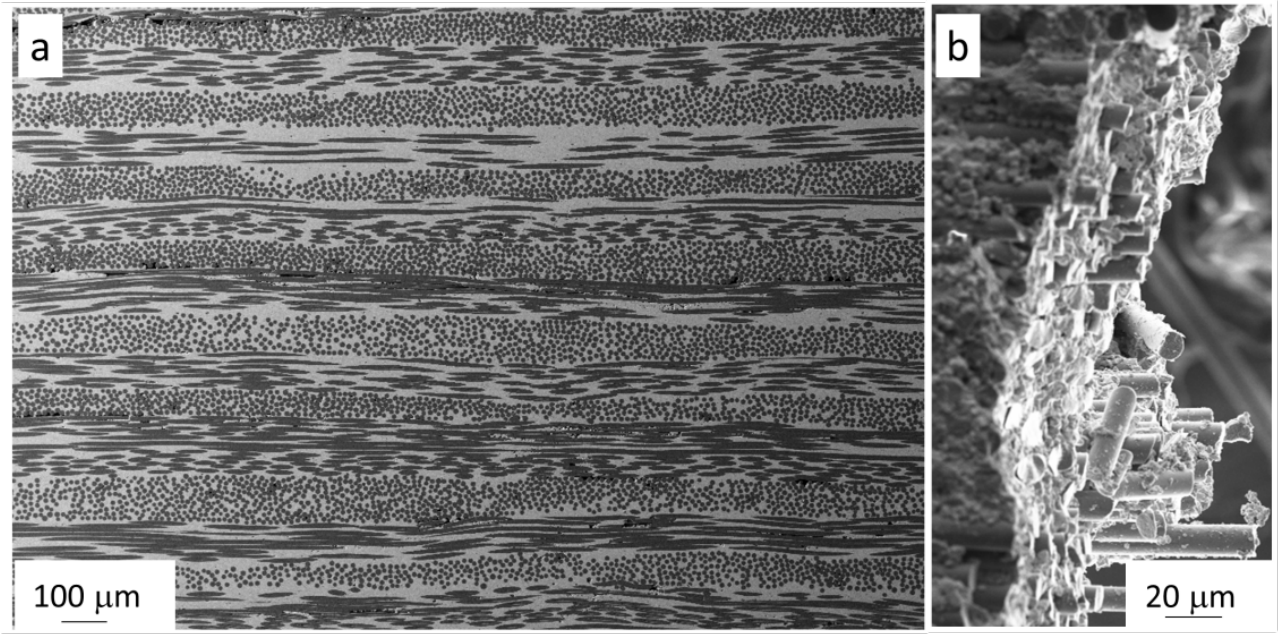

Fig. 3: a) Polished section of samples with 1D infiltrated layers (such as 1D-1450), b) detail of a typical fracture surface of the same.

Figs. 4a,c and b,d compare the matrix/fiber boundary region after sintering at 1450 and 1600°C, respectively. It can be seen that at 1450°C the fiber/matrix interface is clean, Fig. 4a,c, whilst at 1600°C the development of a dark contrasting layer is well evident, Fig. 4b,d. According to previous studies [18] the matrix/fiber interface in similar systems was found to be free from intergranular amorphous films. On the other hand, the presence of dark rims in the fracture image, Fig. 4d, suggests a reprecipitation of Zr-containing SiC phases onto the original SiC grains constituting the fiber, indicating the commencement of a grain growth phenomenon.

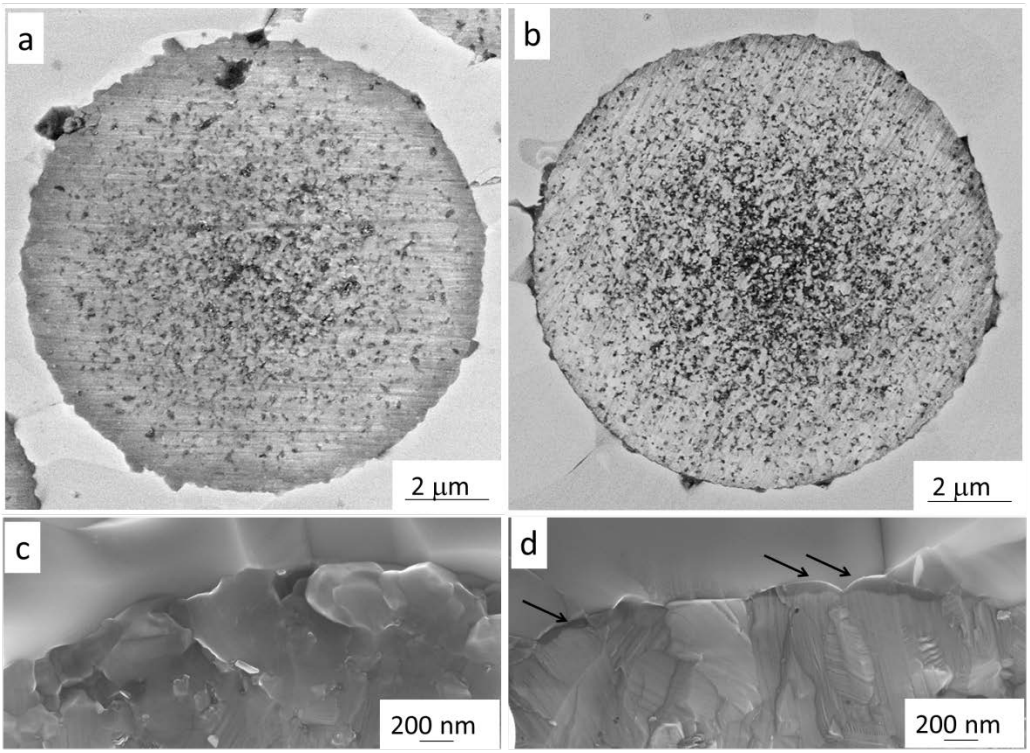

Fig. 4: Particular of the matrix/fiber interface in sample sintered at 1450°C a) Polished and c) fracture surface and c), and sintered at 1600°C b) polished and d) fracture surface

3.2 Mechanical properties and oxidation behavior

Flexural strength values (Table 1) presented a quite scattered range of values, varying from 20 MPa, when using 2D preforms, to 160 MPa, in case of 1D preforms. High temperature flexural strength tests were carried out at 1200°C and 1500°C in air only for specimens obtained from 1D preforms. At 1200°C, the strength values (in the range 135-170 MPa), were not significantly different from room temperature values, whilst at 1500°C an obvious decrease to about 110 MPa was observed.

The load displacement response of the bars obtained from 2D and 1D preforms is shown in Fig. 5 at room temperature, 1200 and 1500°C. Inset in Fig. 5a clarifies the loading configuration with respect to the composite architecture. As reported in Table 1, the room temperature strength of 2D-1550 has a very low value, e.g. 21 MPa with an error over 13 %, due to the presence of large cracks in the matrix and poor infiltration. Fracture very likely initiated at relatively low loads from pre-existing matrix cracks (Fig. 2). Worthy to note, the poor infiltration let to extensive pullout that resulted in a graceful fracture mode, as shown in Fig. 5a.

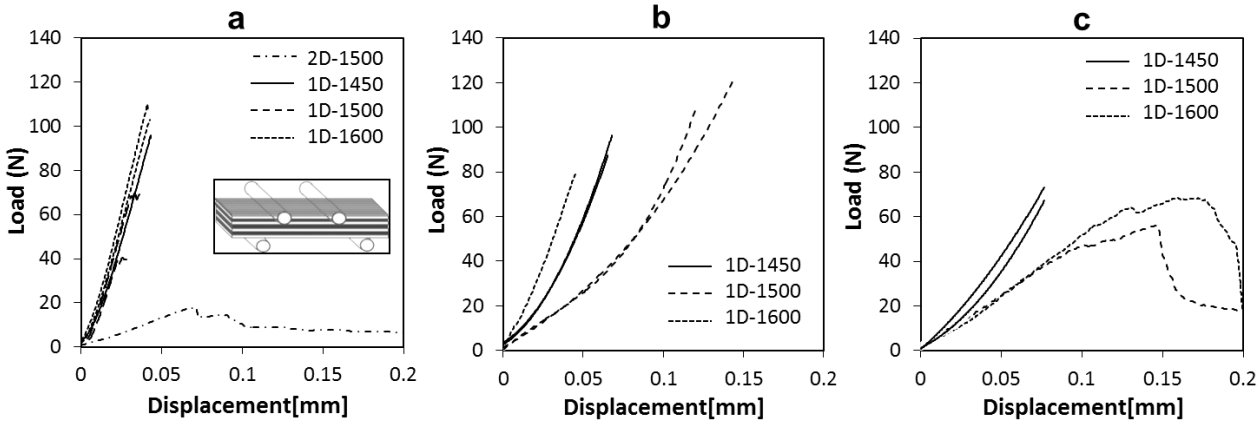

Fig. 5. Load displacement curves for strength test at a) room temperature, b) 1200 and c) 1500°C.

On the contrary, for samples obtained from a 1D preform with a laminate 0-90° structure, strength values ranged from 90 to 160 MPa, with no clear dependence of the strength on the sintering temperature. But in most cases, the load-displacement curves were linear up to fracture, Fig. 5a. For sample 1D-1500, the low value of room temperature strength could also be due to macroscopic infiltration defects that were identified in the bar section (not shown). Other sources of defects come from machining of bars from the sintered tiles. Due to non-perfect alignment of laminate planes, the bar surface was often a patchwork of areas with fibers parallel and perpendicular to the loading direction (see Fig. 6).

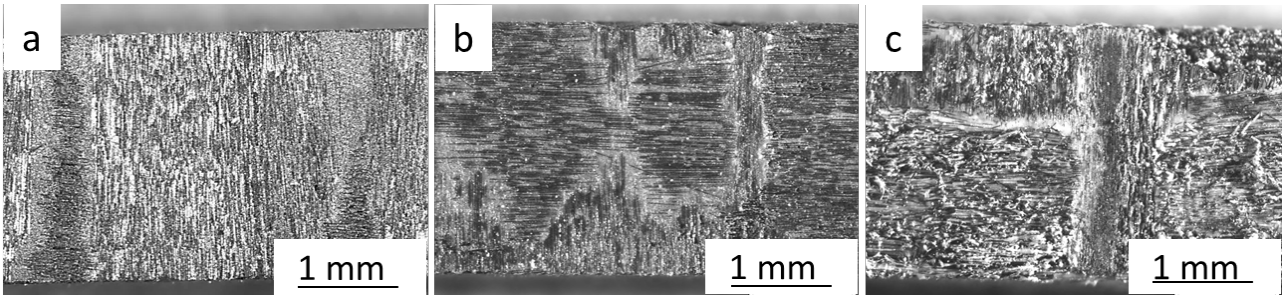

Fig. 6: Optical micrographs of a bar surface, after tests at a) room temperature, b) 1200 °C in air, c) 1500°C in air, showing the irregular surface texture and oxidation phenomena in b and c due to air exposition.

High temperature flexural strength tests were carried out at 1200°C and 1500°C in air for samples 1D-1450, 1D-1500 and 1D-1600. At 1200°C, the strength values (in the range 135-170 MPa) were similar to or even higher than room temperature ones, with no dependence on the sintering temperature. The load-displacement curves were linear up to fracture. The external surface of the specimens resulted covered by a non- continuous silica glass (see the optical

micrograph in Fig. 6b). The cross sections were analyzed by FESEM (not shown) and displayed a subsurface modified layer with an approximate thickness of 10-20 μm where ZrO_2 crystals are visible as well as silica deriving from fiber oxidation. It must be recalled that the bars before rupture are kept inside the air furnace for about two hours. Silica resulting from fiber oxidation diffuses towards the surface. Very likely, the formation of this layer sealed surface defects, which resulted in an increase of strength from 90 to 170 MPa especially for tests at 1200°C. Strength tests at 1500°C confirmed an obvious decrease of strength, probably due to new defects induced by oxidation which overcame the native strength limiting flaws. Optical micrographs of the bar surface confirmed a notable increase of the surface roughness (see Fig. 6c) due to oxide growth and uplifting of fibers in the external layer. All the values were in the range 110-115 MPa, irrespective of the different sintering temperature.

It is also worthy to note that the load displacement curves of samples sintered at 1500 and 1600°C were non linear, with small drops and decrease of the slope (Fig. 5). After the tests, the bars were slightly plastically deformed. On the contrary, load-displacement curves of samples sintered at 1450°C were linear up to fracture. Even if more tests should be performed, this behavior indicates a lower brittleness for samples consolidated at higher temperatures (1D-1500, 1550, 1600). The fresh cross sections of the samples tested at 1500°C (Fig. 7 a,b) reveal that the surficial silica layer was about 10-20 μm thick and the subsurface layer was 60-80 μm deep. Moreover, it was observed that in the initial stage of oxidation at 1500°C a detachment of the fiber from the ZrO_2 matrix occurred, e.g. an oxidation-induced fiber pullout [21], which could be the reason for the small drops observed in the load-displacement curves.

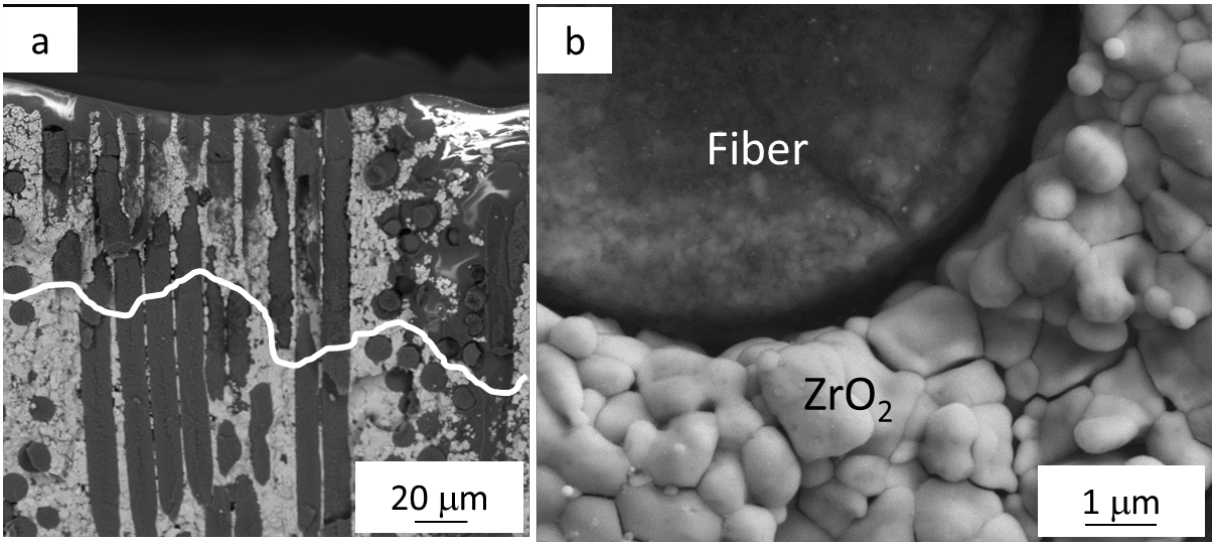

Fig. 7: a) Fresh cross section of bars tested at 1500 in air, b) detachment of the fiber from the oxidized matrix.

It is interesting to compare these data with available literature data on similar composites with short fibers. 4-pt bending strength of ZrB_2 composites with SiC chopped fibers show a strength decrease with increase of the fibers content [16]. We recently measured a value of 170 MPa for ZrB_2 with 50 vol% SiC chopped fibers, which is very close to the present materials, see Table 1. As for the high temperature tests, ZrB_2-15 vol% SiC chopped fiber composites with Tyranno fibers had a strength of 110 MPa at 1500°C, as for the present composites [21]. On the other hand, for C_f/SiC -ZrB_2 composites with a ZrB_2 content of 25vol% the 3-pt bending strength was 160 MPa [15], whilst the SiCf-ZrB_2-SiC composite developed by Levine et al [8] composites exhibited a 4-pt bending strength of 130 MPa at room temperature that decreased to 85 MPa at 1330°C in air, probably due to residual porosity.

Oxidation behavior significantly varied as a function of the starting preform, revealing a much higher degradation for samples obtained from 2D preforms, in spite of the same starting compositions/fiber volumetric amount.

The composites response to high temperature (1650°C) exposure in air is testified in the cross section images of Fig. 8 a,b. The low level of infiltration of sample 2D-1500 caused excessive sensitivity to oxidation, revealing an oxygen penetration down to 300 μm from the surface (Fig. 8a), with formation of ZrO_2 and progressive detachment of oxidized fiber-rich regions from oxidized matrix-rich regions. On the contrary, when a satisfactory integration of the constituent phases was achieved, the oxidized subsurface layer was less than 80 μm deep (Fig. 8b). Worthy to note, the silica surface layer was essentially due to oxidation of SiC fibers to SiO_2 and diffusion to the sample surface and this had the consequence to leave holes in the subsurface layer.

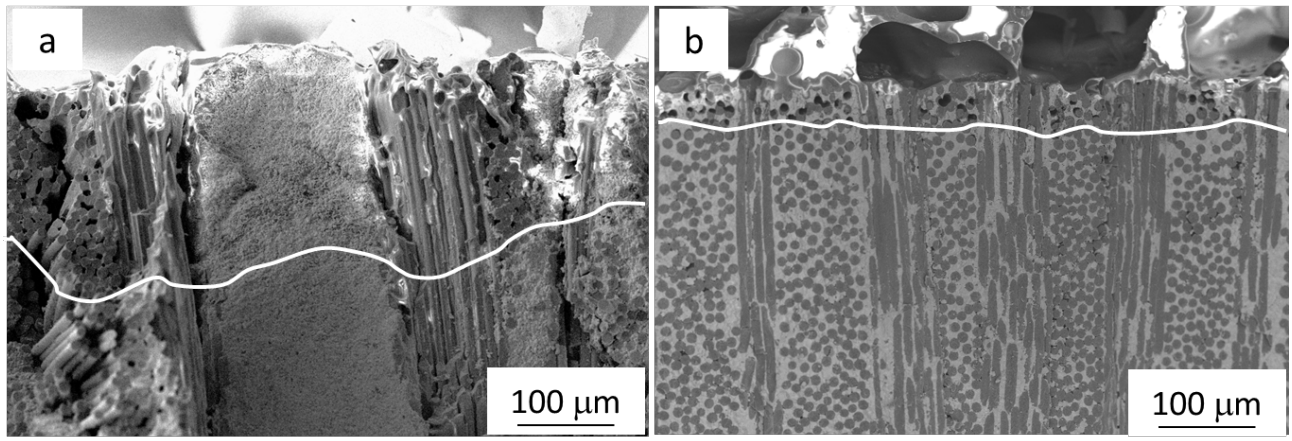

Fig. 8. Oxidation tests in bottom-loading furnace at 1650°C for 5 min. a) sample 2D-1500, b) sample 1D-1450. The white line divides oxidized layers from the unreacted bulk.

4. Conclusions

This study demonstrates the feasibility of SiC continuous fiber reinforced ZrB_2 coupling a conventional infiltration technique with hot pressing. The SiC-ZrB_2 composites have bulk densities in the range 4-4.2 g/cm^3, with limited porosities, < 10 %, but the sample homogeneity is affected by the type of preform. The infiltration degree was very poor for 2D preforms but excellent for 1D preforms with a 0-90° architecture. Nearly full densification was accomplished at 1450°C with low effect of the sintering temperature on microstructure and strength, even if increasing the sintering temperature caused a change in the fiber morphology with grain growth phenomena. With uncoated fibers, a strong fiber-matrix interface developed, which inhibited the fiber pullout. Flexural strength values of 1D infiltrated samples were around 150 MPa at room temperature, in the range 135-170 MPa at 1200°C and 110 MPa at 1500°C in air. Load-displacement curves recorded during flexural strength tests were linear up to fracture up to 1200°C. Oxidation – induced fiber pullout and non linear load-displacement behavior were observed during strength tests at 1500°C in air. Short term oxidation tests at 1650°C confirmed the importance of an homogenous integration between the constituent phases (matrix and fibers) in order to ensure a proper oxidation resistance. The oxidized layers were 300 μm deep for poorly infiltrated 2D samples, and 80 μm for well infiltrated 1D samples.

Acknowledgements

Authors wish to thank D. Dalle Fabbriche, A. Piancastelli, A. Natali Murri for technical support.

1. Bansal, N.P. (Ed.) Handbook of ceramic composites, Kluwer Academic publisher, 2005.
2. Krenkel W. (Ed.), Ceramic Matrix Composites – Fiber Reinforced Ceramics and Their Application, Wyley-VCH Verlag, Weinheim, 2008.
3. Fahrenholtz WG, Hilmas GE, Talmy IG, Zaykoski JA. Refractory Diborides of Zirconium and Hafnium. J Am Ceram Soc 2007;90:1347–64.
4. Opeka, MM, Talmy IG, Zaykoski JA. Oxidation-based materials selection for 2000°C + hypersonic aerosurfaces: Theoretical considerations and historical experience. J Mater Sci 2004;39:5887-904.

5. Guicciardi S, Silvestroni L, Nygren M, Sciti D. Microstructure and toughening mechanisms in spark plasma sintered ZrB_2 ceramics reinforced by SiC whiskers or SiC chopped fibers. J Am Ceram Soc 2010;93:2384-91
6. Sciti D, Pienti L, Natali Murri A, Landi E, Medri V, Zoli L. From random chopped to oriented continuous SiC fibers-ZrB_2 composites. Mat & Des 2014;63:464–70.
7. Leslie CJ, Boakye EE, Keller KA, Cinibulk MK. Development and Characterization of Continuous SiC Fiber-Reinforced HfB_2-based UHTC Matrix Composites using Polymer Impregnation and Slurry Infiltration Techniques. Int J Appl Ceram Technol 2015;12:235-44.
8. Levine S R, Opila EJ, Halbic MC, Kisera JD, Singh M, Salema JA. Evaluation of ultra-high temperature ceramics for aeropropulsion use. J Eur Ceram Soc 2002;22:2757-67.
9. Paul A, Jayaseelan DD, Venugopal S, Zapata-Solvas E, Binner J, Vaidhyanathan B, Heaton A, Brown P, Lee WE. UHTC composites for hypersonic applications. Am Ceram Soc Bull 2012;91:22-9.
10. Jayaseelan D-D, Guimaraes de Sa R, Brwon P, Lee WE. Reactive infiltration processing (RIP) of ultra high temperature ceramics (UHTC) into porous C/C composites tubes. J Eur Ceram Soc 2011;31:361-8.
11. Li Q, Dong S, Wang Z, Zhou PH, Yang J, Wu B. Fabrication and Properties of 3-D Cf/SiC–ZrC Composites, Using ZrC Precursor and Polycarbosilane. J Am Ceram Soc 2012;95:1216–19.
12. Li Q, Dong S, Wang Z, Shi G, Fabrication and properties of 3-D Cf/ZrB2-ZrC-SiC composites via polymer infiltration and pyrolysis. Ceram Int 2013;39:5937- 41.
13. Wang Y, Liu W, Cheng L, Zhang L. Preparation and properties of 2D C/ZrB_2-SiC ultra high temperature ceramic composites. Mat Sci Engng A 2009;524:129-33.
14. Li L, Wang Y, Cheng L, Zhang L. Preparation and properties of 2D C/SiC-ZrB_2-TaC composites. Ceram Int 2011;37:891-96.
15. Hu H, Wang Q, Chen Z, Zhang C, Zhang Y, Wang J. Preparation and characterization of C/SiC-ZrB_2 composites by precursors infiltration and pyrolysis process. Ceram Int 2010;36:1011-16.
16. Sciti D, Silvestroni L, Saccone G, Alfano D. Effect of different sintering aids on thermomechanical properties and oxidation of SiC fibers Reinforced ZrB_2 composites. Mat Chem & Phys 2012;137:834-42.
17. Medri V, Capiani C, Gardini D. Slip Casting of ZrB_2-SiC Composite Aqueous Suspensions. Adv Eng Mat 2010;12:210-15.

18. Sciti D, Silvestroni L, Medri V, Monteverde F. Sintering and densification of ultra-high temperature ceramics, in: Ultra-High Temperature Ceramics: Materials for Extreme Environment Applications, eds Fahrenholtz W., Wuchina E., Lee W., and Zhou Y., ISBN 0-471-9781118700785 Copyright © 2014 Wiley, Inc.
19. Ishikawa T. Advances in Inorganic fibers. Adv Poly. S., 2005;178:109-44.
20. Silvestroni L, Dalle Fabbriche D, Sciti D. Tyranno SA3 fiber–ZrB_2 composites. Part I: Microstructure. Mat & Des 2014;65:1253-1263.
21. Silvestroni L, Dalle Fabbriche D, Sciti D. Tyranno SA3 fiber–ZrB_2 composites. Part II: Microstructure. Mat & Des 2014;65:1264-1273.
22. Mallik M, Kailath AJ, Raya KK, Mitra R. Electrical and thermos-physical properties of ZrB_2 and HfB_2 based composites. J Eur Ceram Soc 2012;32:2545–55.